ELSEVIER

Physica C 319 (1999) 197–208

PHYSICA C

Relationship among synthesis, microstructure and properties in sinter-forged Bi-2212 ceramics

V. Garnier [a,*], R. Caillard [b], A. Sotelo [a], G. Desgardin [a]

[a] *Laboratorie CRISMAT, 6, Bd. du Marechal Juin, 14050, Caen cedex, France*
[b] *Laboratoire LERMAT, 6, Bd. du Marechal Juin, 14050, Caen cedex, France*

Received 23 February 1999; received in revised form 4 May 1999; accepted 5 May 1999

Abstract

High quality Bi-2212 powders were prepared using three different synthetic methods (solid state, sol–gel and polymer matrix), showing that the polymer matrix method is very promising from the point of view of the synthesis time and grain size. The Bi-2212 sintered pellets were then submitted to sinter-forging process to obtain textured ceramic discs. The discs were characterized by XRD, pole figures and SEM to determine the phase purity, the texture degree and the microstructure, respectively. Following characterization, the discs were cut into bars and annealed for 12 h at different temperatures ranging between 845 and 873°C to determine the best thermal treatment, whereafter they were characterized using resistivity and transport J_c measurements. It has been found that most of the bars had a T_c around 92 K and that transport properties can be correlated to the samples' microstructure. © 1999 Elsevier Science B.V. All rights reserved.

Keywords: Synthesis; Bi-2212; Sol–gel; Microstructure

1. Introduction

Since Raveau's discovery [1] and Maeda et al.'s work [2] on superconductivity in the Bi–Sr–Ca–Cu–O (BSCCO) system (in the absence of rare earth elements, while still obtaining high T_c values), significant effort has been focused towards the development of synthetic procedures which lead to single-phase ceramics with a well-defined T_c.

The BSCCO system, in spite of a large decrease of J_c in high magnetic field, has some important advantages over the well known 1,2,3 superconductor RE-Ba–Cu–O systems (RE = rare earth): (a) in some of the samples, higher T_c values can be obtained [2–5]; (b) the elimination of rare earths leads to lower costs of the final material [3]; and (c) lower reactivity to moisture [6].

Three superconducting BSCCO phases with $Bi_2Sr_2Ca_{n-1}Cu_nO_{2n+4+\delta}$ stoichiometries, where $n = 1$, 2 and 3, with T_c values around 10, 90 and 110 K, respectively, have been synthesized and well characterized. These three phases will be referred to as Bi-2201 ($n = 1$), Bi-2212 ($n = 2$) and Bi-2223 ($n = 3$) [5–8]. The synthesis of pure Bi-2201 and Bi-2212 phases in this system is relatively easy, while synthesis of single phase Bi-2223 has been shown to be a difficult task [9] and this can be better

* Corresponding author. Tel.: +33-2-31-45-29-15; E-mail: garnier@crismat.ismra.fr

0921-4534/99/$ - see front matter © 1999 Elsevier Science B.V. All rights reserved.
PII: S0921-4534(99)00308-1

understood on the basis of previously published phase diagram studies in air [10].

The next goal in the Bi ceramics consists on the enhancement of the transport critical current (J_c). In order to achieve this objective, many techniques were used with good performance, such as thin [11,12] and thick [13] film technology, wires and tapes by the PIT method [14], and texturation using the Bridgman [15] or laser floating zone [16,17] methods. Another method, the hot uniaxially pressing technique [18,19], has also been used to successfully obtain bulk monoliths of high-T_c superconductors with a grain oriented texture. By sinter-forging a pelletized specimen, it is possible to orient the *c*-axis of the different crystals along the press axis to increase J_c along the *ab* plane. Studies relating hot-pressing processes [20–24] have already been carried out with different pressing and heat treatment conditions which showed the efficiency of the texturing method. However, the final result is also dependant on the synthetic route of the precursor and therefore cannot be compared due to different sinter-forging conditions.

To perform the sinter-forging process, we have chosen to work under partial decomposition of Bi-2212, corresponding to the incongruent melting (partial melting), in order to improve the grain sliding. In fact, if the temperature is too low to obtain a partial melting, the process does not offer the necessary conditions to obtain a high densification and orientation [23], and if the temperature is too high, a melt will be obtained which lead to a glass by quenching [25].

So, in the following work, we have studied the relationship between microstructure and superconducting properties for samples obtained from three different synthetic procedures while maintaining the sinter-forging conditions (initial pressure and temperature) constant.

2. Experimental methods

The Bi-2212 powders, with the nominal composition $Bi_2Sr_2CaCu_2O_{8+\delta}$, used for this study were prepared by the following three methods.

(a) *Solid state reaction*: Bi_2O_3 (99 + %, Rectapur), $SrCO_3$ (99 + %, Rectapur), $CaCO_3$ (99 + %, Rectapur) and CuO (99 + %, Normapur) were attri-

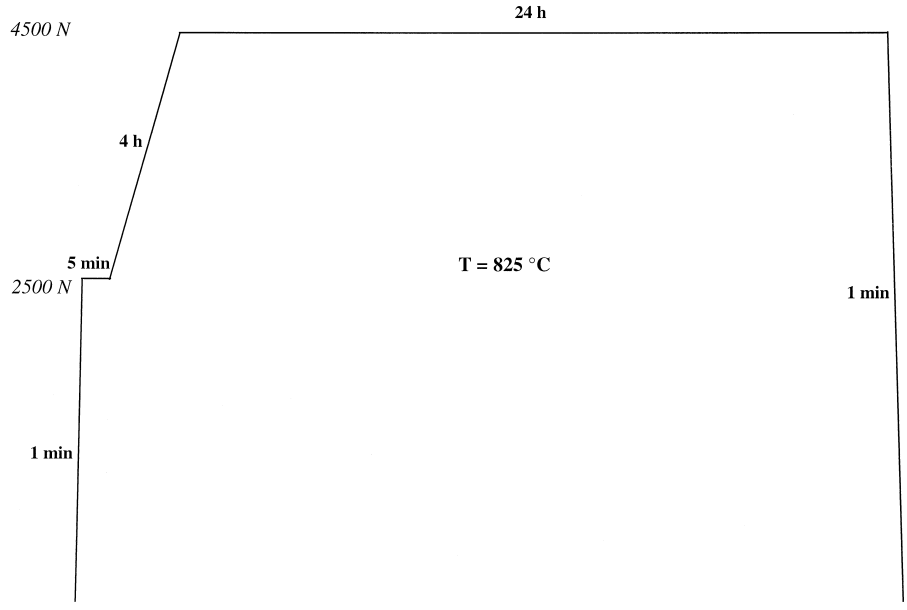

Fig. 1. Schema of the sinter-forging cycle pressure versus time performed on sintered Bi-2212 pellets at 825°C.

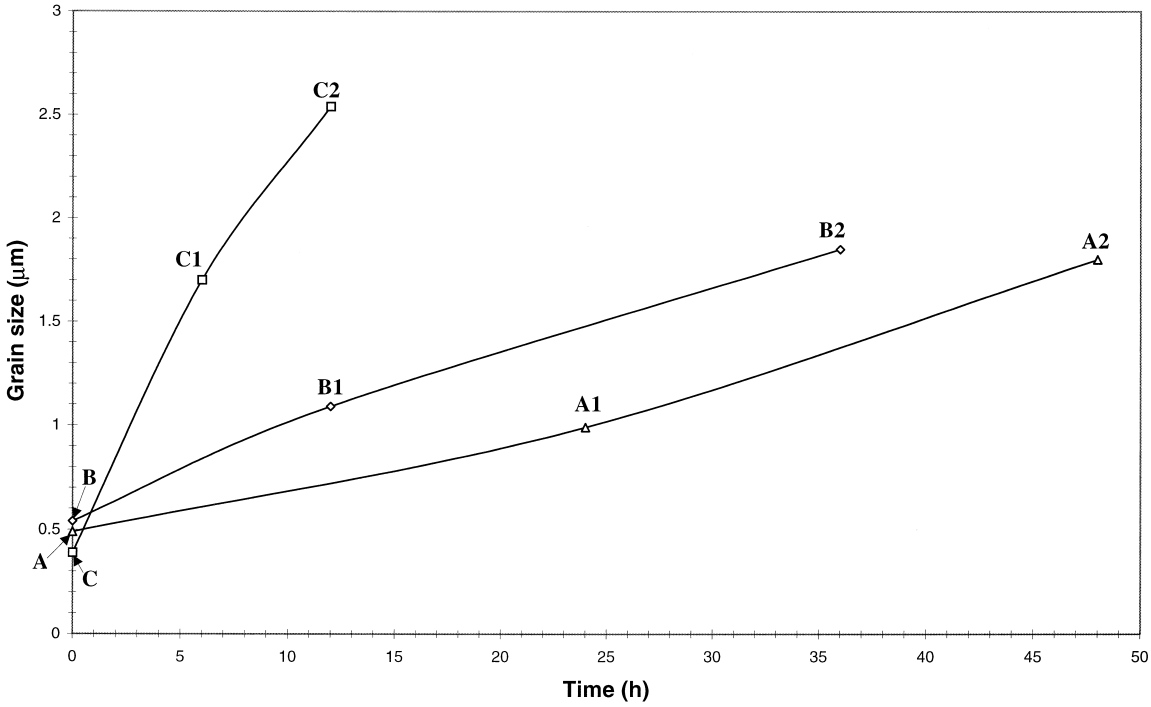

Fig. 2. Grain size evolution vs. each calcination time for samples obtained by (A, A1 and A2) solid state, (B, B1 and B2) sol–gel, and (C, C1 and C2) polymer matrix methods, before calcination, and after the first and second calcination processes, respectively.

tor milled in an inert medium using zirconia balls and absolute ethanol for 1.5 h at 800 rpm. The resulting suspension was dried using IR radiation and subsequently placed in an oven at 120°C for 12–24 h to evaporate the maximum amount of ethanol. The resulting powder was then passed through a 125 μm sieve. Then, as proposed by Majewski et al. [26], the powder was calcined in two steps, the first at 750°C for a period of 24 h, whereafter it was milled by hand in an agate mortar, and then calcined a second time at 800°C for 24 h and then milled again. These two thermal treatments insure the total evaporation of the ethanol as well as the decomposition of the alkaline earth carbonates.

Table 1
Summary of the main characteristics of the three investigated processings

Synthetic procedure	Calcination process	Particle size (μm)	Sintering process	Best T_c/annealing temperature	Best J_c/annealing temperature/T_c/cross section/voltage contact distance
Solid state	Before	0.49			
	750°C, 24 h +	0.99			
	820°C, 24 h	1.80	820°C, 24 h	92.4 K/863°C	1500 A cm^{-2}/855°C/90.9 K/(1.56 * 0.78) mm/10 mm
Sol–gel	Before	0.54			
	750°C, 12 h +	1.09			
	820°C, 24 h	1.85	845°C, 24 h	92.8 K/860°C	1200 A cm^{-2}/873°C/90.3 K/(1.5 * 0.86) mm/10 mm
Polymer	Before	0.39			
matrix	750°C, 6 h +	1.70			
	800°C, 6 h	2.54	845°C, 12 h	91.9 K/850°C	200 A cm^{-2}/850°C/91.9 K/(1.5 * 0.6) mm/10 mm

The powder is then isostatically pressed at 350 MPa in the form of a bar, sintered at 820°C for 24 h, milled, uniaxially pressed at 200 MPa in the form of pellets (16 mm diameter, ~ 3 g) and sintered again at 820°C for 24 h.

(b) *Sol–gel method* [27,28]: CuO (Prolabo Normapur, 99%), Bi_2O_3 (Prolabo Rectapur, 99 + %), $SrCO_3$ (Prolabo Rectapur, 99 + %) and $CaCO_3$ (Prolabo Rectapur, 99 + %) were dissolved in a mixture of distilled water and nitric acid (Carlo Erba, 65%) to obtain a light pale blue solution. A second solution of ethylenediaminetetracetic acid (EDTA, Prolabo, 98%) in aqueous ammonium hydroxide (Prolabo Normapur, $NH_3 > 28$ wt.%) was prepared using a molar ratio necessary to raise the pH of the solution to a value of 11 in order to dissolve the EDTA.

The first solution is then added dropwise to the second one, which caused the mixture to turn dark blue immediately. In some cases an excess of nitric acid (added to totally dissolve the remaining Bi_2O_3) is needed, and in the resulting solution a white EDTA precipitate forms due to the decrease of the pH; however, the precipitate easily redissolved by adding more ammonium hydroxide to raise the pH to a value between 6 and 10.

The final solution is then heated on a hot plate to reduce the volume. During this process, the addition of ammonium hydroxide may be necessary to maintain the pH above 6 to avoid precipitation of the EDTA.

When the solute concentration increases (i.e., approximately 50 g of the initial precursors per 100 ml of remaining solution left) the color of the mixture turned dark green. It should be noted that in this step, pH control is critical in order to avoid precipitations.

Further heating transforms the solution into a gel that subsequently transforms into a dark-brown foam. At this point it is necessary to increase the temperature to create a self-combustion of the foam which causes a release in a high volume of volatile vapours (water, CO_2 and NO_x), subsequently leaving a dark-brown precursor powder. This precursor is then heated up to 750°C for 12 h to decompose the remaining organic material.

This powder is then milled in an agate mortar and calcined at 820°C for 24 h. After cooling, the remaining powder was ground and pelletized (200 MPa, 16 mm diameter, ~ 3 g) and sintered at 845°C for 24 h.

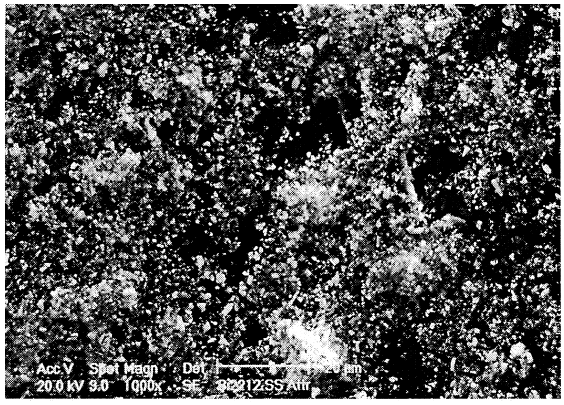

A

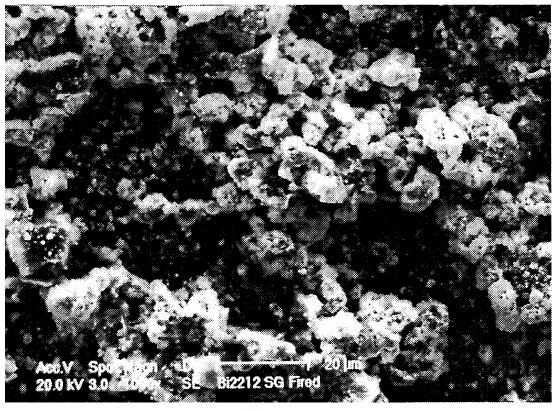

B

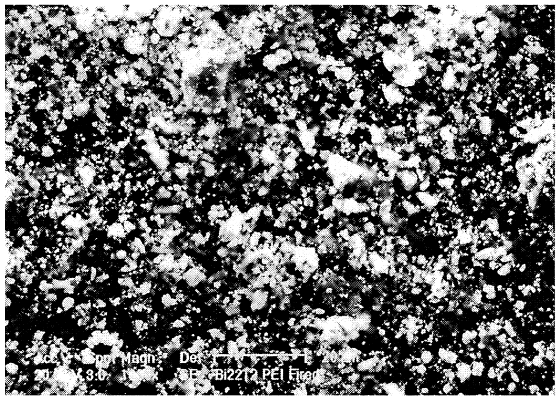

C

Fig. 3. SEM micrographs of precursor powders before the calcination process for (A) solid state after attritor milling, and (B) sol–gel and (C) polymer matrix methods after firing.

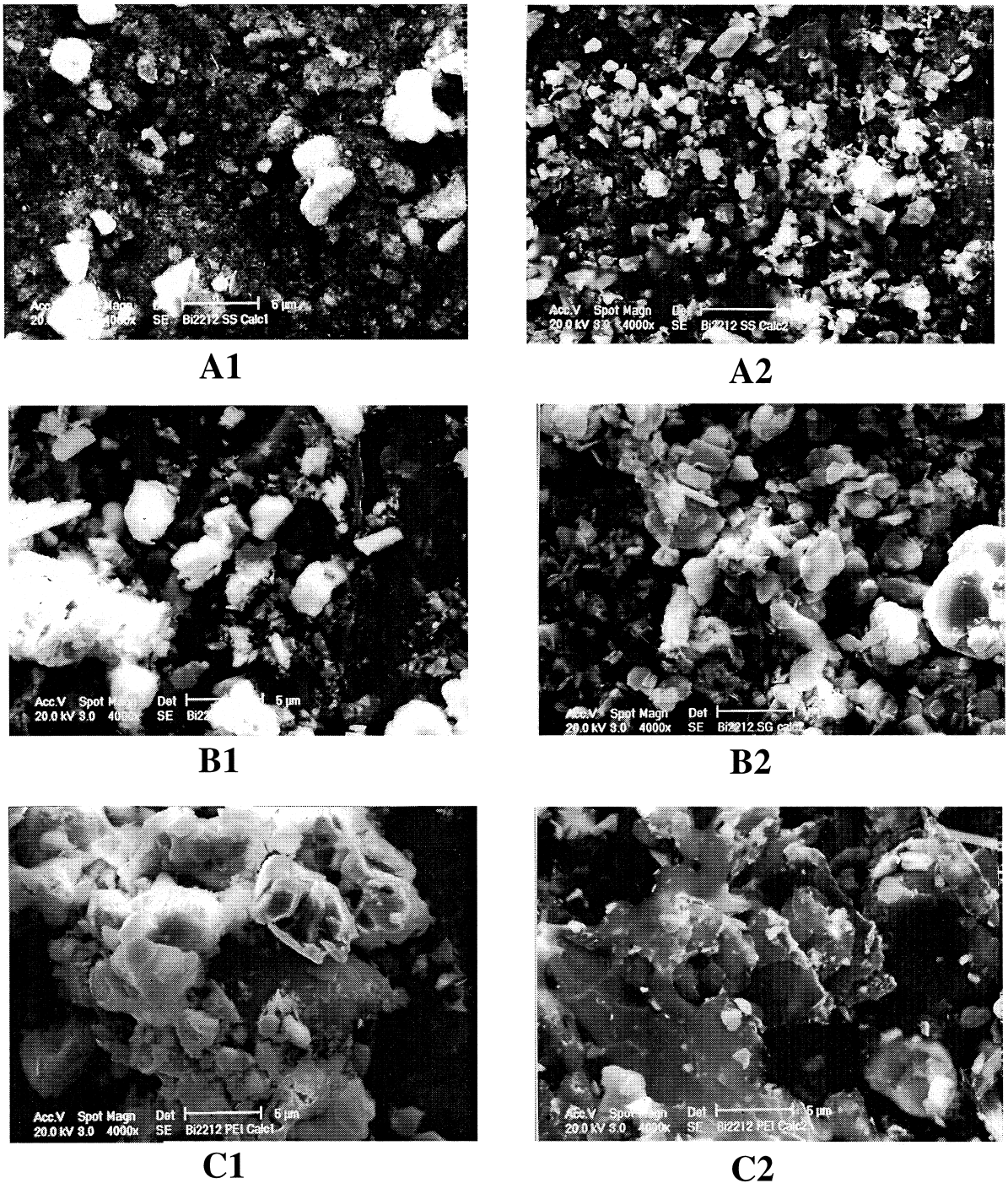

Fig. 4. SEM micrographs of precursor powders, showing the grain size evolution for (A1 and A2) solid state, (B1 and B2) sol–gel, and (C1 and C2) polymer matrix methods after first and second calcination processes for each method, respectively.

(c) *Polymer matrix method*: $Bi(CH_3COO)_3$ (Aldrich, 99.99 + %), $Sr(CH_3COO)_2 \cdot 1/2H_2$ (Aldrich, 99.9%), $Ca(CH_3COO)_2 \cdot H_2O$ (Aldrich, 99 + %) and $Cu(CH_3COO)_2 \cdot H_2O$ (Aldrich, 98 + %) were dissolved in a mixture of acetic acid (SDS, 99%) and distilled water to obtain a pale blue solution. To this solution, another solution of polyethyleneimine (PEI Aldrich, 50 wt.% H_2O) in distilled water was added and the resulting solution turned royal blue immediately. This dark blue solution was then introduced into a rotary evaporator to reduce the volume to approximately 10% of the initial volume. The concentrated solution is then introduced into a crucible and placed on a hot plate, increasing slowly the temperature until total evaporation of the solvent occurs. The thermoplastic paste that forms was subsequently fired on a hot plate at approximately 400°C. Due to the exothermic reaction which takes place, the temperature of the crucible, measured with an IR pyrometer (Williamson 9220PS-S-C), is around 750°C.

As proposed by Sotelo [17], the resulting powder is then milled in an agate mortar and calcined in two steps, the first at 750°C for 6 h and the second at 800°C for 6 h with an intermediate milling. After cooling, the remaining powder is ground, pelletized (200 MPa, 16 mm diameter, ~ 3 g), and sintered at 845°C for 12 h.

After obtaining the 2212 phase, a sinter-forging process under air using silver foil on alumina pieces to avoid contact between the piston and the superconducting ceramic was performed on sintered pellets at a temperature of 825°C measured with a Pt–PtRh thermocouple placed close to the sample, as described in Fig. 1. This temperature is theoretically lower than the melting temperature for the 2212 phase (~ 880°C), but it has produced a small amount of liquid phase (partial decomposition) due to the applied pressure. The sinter-forged pellets were cut into bars 1.5 mm wide which were then annealed for 12 h at different temperatures between 845 and 873°C under air.

Powder XRD (Philips PW3710, $\lambda_{Cu}[K_{\alpha 1}]$), granulometry (Malvern mastersizer) and SEM (Philips XL 30) measurements were performed throughout the synthetic procedure, using the same conditions for all the samples, to characterize the intermediate products as well as to determine the phase purity in the final sintered products. The samples for granulometry measurements have been prepared by ultrasonic

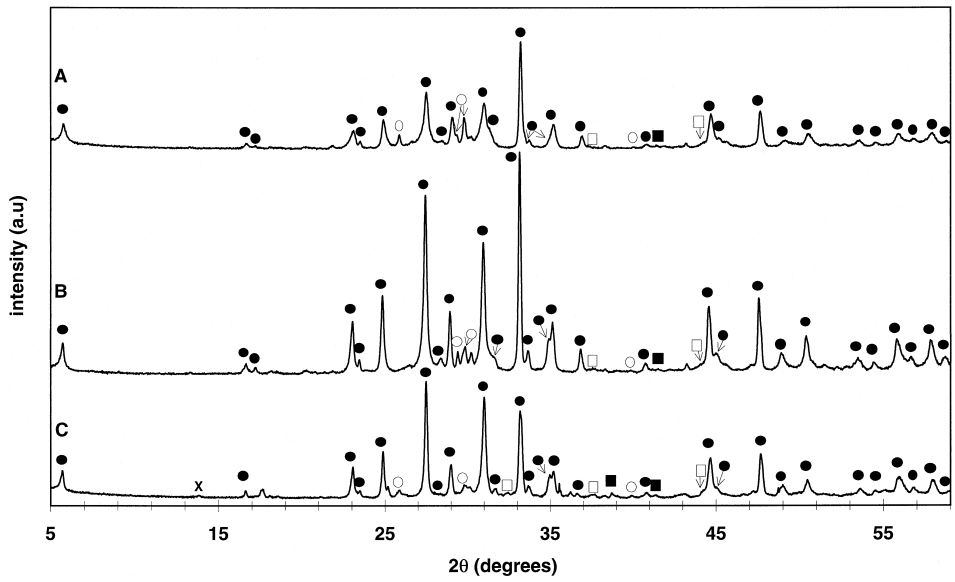

Fig. 5. X-ray diffraction after the second calcination step for samples obtained by (A) solid state, (B) sol–gel and (C) polymer matrix methods. The symbols correspond to: ● 2212, ○ 2201, × Ca_2CuO_3, □ $CaCu_2O_3$, and ■ CuO.

mixing in acetone to insure the breaking of the agglomerates, to avoid their influence on the grain size.

In order to characterise the sinter-forged materials XRD (Seifert XRD 3000 P), pole figures (Philips Xpert) and SEM (Philips XL 30) observations were made to study the grain orientation. Transport J_c and resistivity measurements were performed to determine the electrical properties of each of the annealed bars.

3. Results and discussion

3.1. Synthesis of 2212

Fig. 2 and Table 1 show the grain size evolution versus calcination time for all three synthetic procedures. For all three methods the precursors have approximately the same grain size before the first calcination step. It can be clearly seen that the grain growth rate is much higher in the polymer matrix method than for the other two synthetic methods. Fig. 3 shows the SEM micrographs of those precursors before calcination. It can be observed that, as a consequence of its preparation, solid state powder (A) is formed by a mixture of small grains of carbonates and metallic oxides, while the other two powders show the presence of agglomerates, relatively big and porous in the case of sol–gel (B), and smaller and compact for the polymer precursor (C). The evolution of the grain size during calcination shown in Fig. 2 is confirmed by SEM observations (Fig. 4) by which improvement of crystallinity and differences in particles sizes between the three methods are demonstrated. The phases obtained after the calcination process were determined by the XRD patterns shown in Fig. 5. It can be clearly seen that in all cases the final products after the calcination processes are predominantly the 2212 phase, with minor amounts of the 2201 phase, and traces amounts of calcium cuprate and CuO phases. The samples obtained by solid state reaction show the poorest crystallinity (broader and less intense peaks on the XRD pattern) even though their thermal treatment was the longest. The samples obtained by the sol–gel method and the polymer matrix method, using the same measurement parameters, show the sharpest XRD peaks (half height width), but all the Bi-2212 (*hkl*) peaks of the sol–gel method are more intense

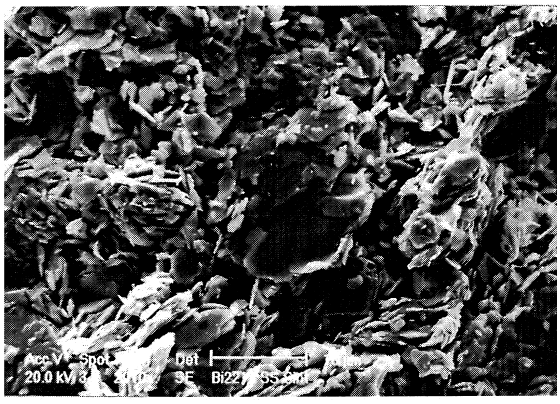

A

B

C

Fig. 6. SEM micrographs of samples after sintering for (A) solid state, (B) sol–gel, and (C) polymer matrix methods.

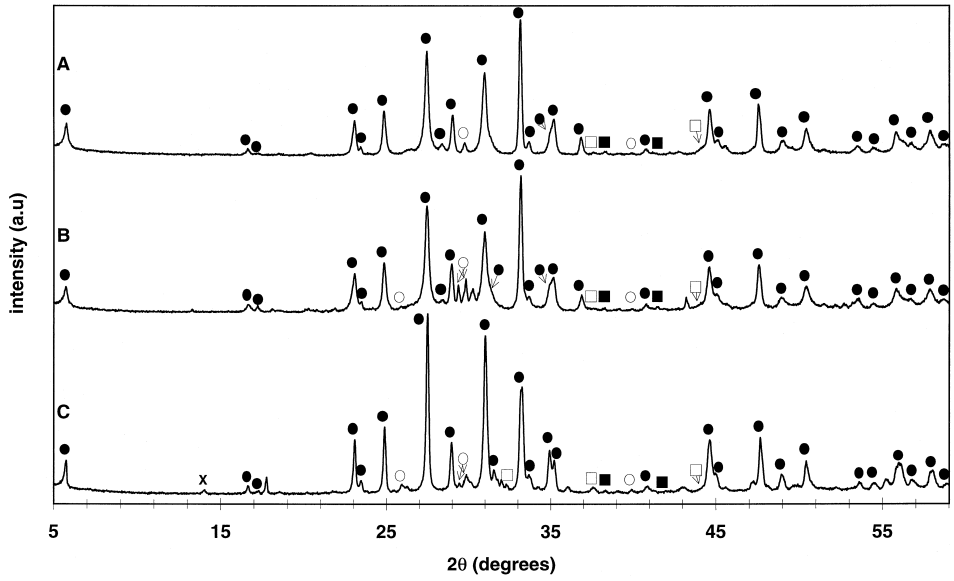

Fig. 7. X-ray diffraction after sintering for samples obtained by (A) solid state, (B) sol–gel and (C) polymer matrix methods. The symbols correspond to: ● 2212, ○ 2201, × Ca_2CuO_3, □ $CaCu_2O_3$, and ■ CuO.

than those obtained with the polymer matrix method, showing that there is no preferential orientation effect, and consequently that the crystallinity is better for the sol–gel method than for the polymer matrix method which correspond to a shorter thermal treatment.

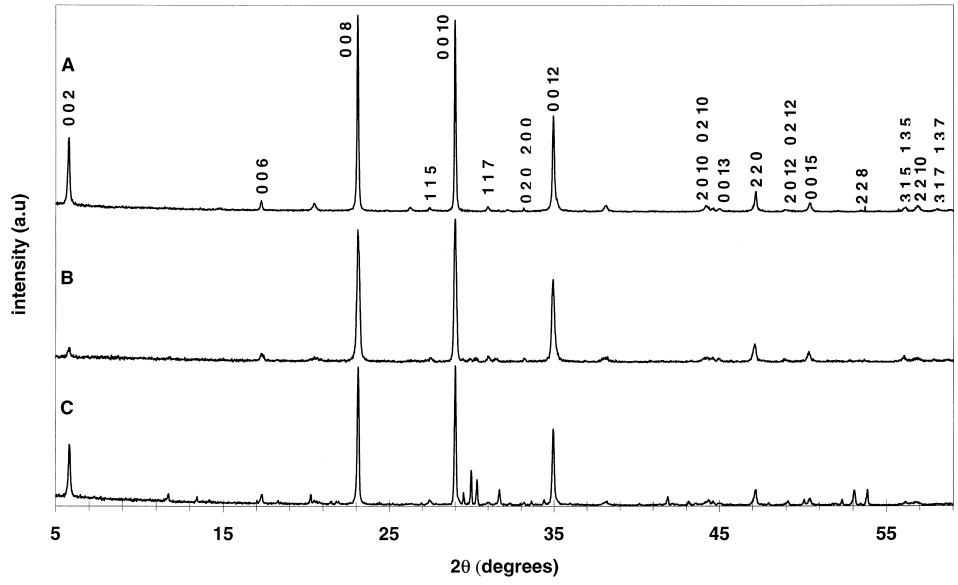

Fig. 8. X-ray diffraction of sinter-forged samples obtained by (A) solid state, (B) sol–gel and (C) polymer matrix methods showing the *hkl* index.

The three calcined precursors were then sintered following the temperature and time parameters listed in Table 1. To characterize the grain size after sintering, SEM was used on fractured samples (see Fig. 6). It can be observed by these micrographs that grains are randomly oriented with a large porosity and that the same kind of evolution was obtained in the calcination steps: larger grains for samples obtained by the polymer matrix method than for those obtained by the other two methods. Nevertheless, as shown by XRD diffraction patterns in Fig. 7, for all three methods we obtained a nearly pure 2212 phase with only minor unknown lines, principally with the polymer method. But this later method leads to a quicker kinetic formation of the Bi-2212 phase, and larger grain size. So, this method seems to be very promising to limit the number of grain boundaries in the forged samples.

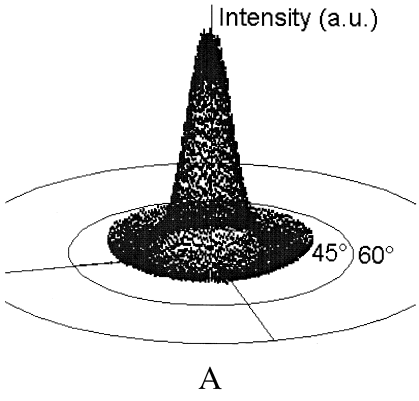

Fig. 9. Pole figures of sinter-forged samples obtained by (B) sol–gel and (C) polymer matrix methods. The diffraction pattern was performed on the (0010) lines.

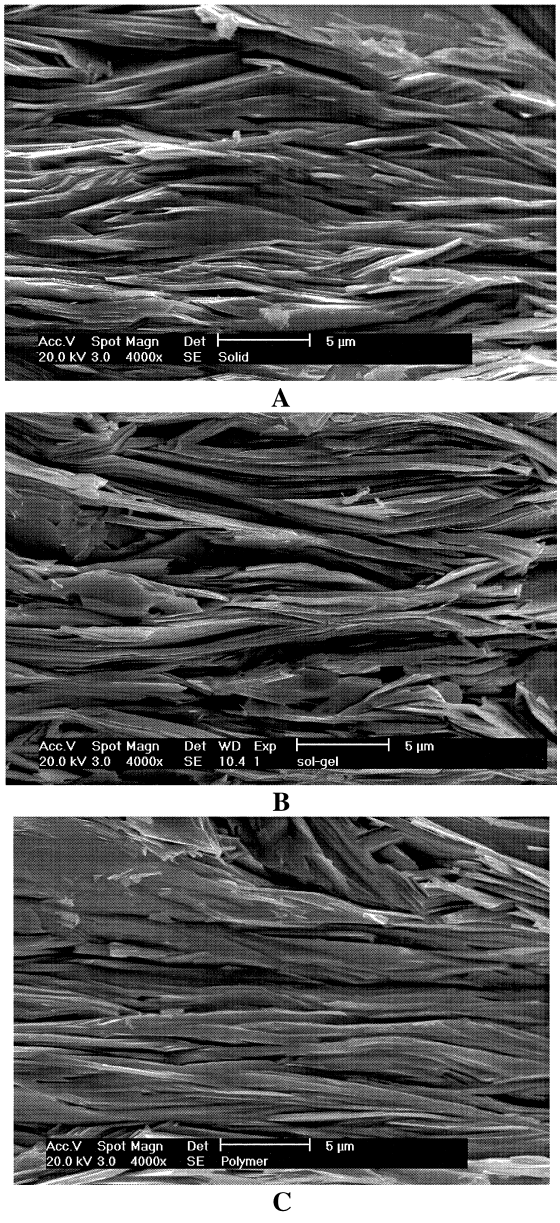

Fig. 10. SEM micrographs of sinter-forged samples obtained by (A) solid state, (B) sol–gel and (C) polymer matrix methods. The arrow shows the direction of the applied pressure.

Also, due to the formation of platelets, which will be reoriented during the sinter-forging process, and due to the better behavior of sintered pellets under

stress compared to unsintered pellets, the samples were adequate enough to perform the texturation process.

3.2. Texturation

After obtaining the Bi-2212 phase for each synthetic procedure, a sinter-forging process was performed on the sintered pellets using a temperature of 825°C under air and a starting pressure of 30 MPa. In these conditions, the sharper and larger diameter pellets correspond to samples obtained by the polymer matrix method ($e \cong 0.6$ mm; $\varnothing \cong 30$ mm), while for the other two methods the deformation is smaller ($e \cong 0.8$ mm; $\varnothing \cong 22$ mm).

Fig. 8 shows the XRD spectra for the sinter-forged materials. It can be seen that for the three methods the Bi-2212 phase is still nearly pure, except in samples prepared by the polymer matrix method that show additional peaks due to the formation of unknown secondary phases along the sinter-forging process. The preferential orientation can be observed by the intensity of the (001) lines, even if weak (hkl) lines reveal that misorientation still remains. The texture degree of the sinter-forged disks has been performed by pole figure measurements using the (0010) line of the Bi-2212 spectra (see Fig. 9). It was found that 50% of the grains are misoriented from the forging axis between 0–14° for the disks obtained by both the sol–gel (B) and solid state (A) method and between 0–17° for those obtained by the polymer matrix method (C). The high sample density and the relatively good texture formation can be seen on the SEM micrographs shown in Fig. 10.

3.3. Superconducting properties

The best T_c for each method was obtained after annealing for different temperatures: 91.9 K at 850°C for the polymer (C), 92.8 K at 860°C for the sol–gel (B), and 92.4 K at 863°C for the solid state (A) methods (see insert on Fig. 11). It is evident from Fig. 11 that the samples obtained by the polymer matrix method had a much higher resistivity value in the normal state than the samples produced by the other two synthetic methods. This result will be discussed in the next paragraph.

The transport critical current density, (J_c), was measured using the standard four points technique at 77 K and 0 T applied magnetic field with the criteria of 1 μV/cm. For the solid state sample, the best J_c value is around 1500 A/cm^2 obtained after annealing at 855°C, 12 h; for the sol–gel sample, 1200 A/cm^2 after annealing at 873°C, 12 h; and for the

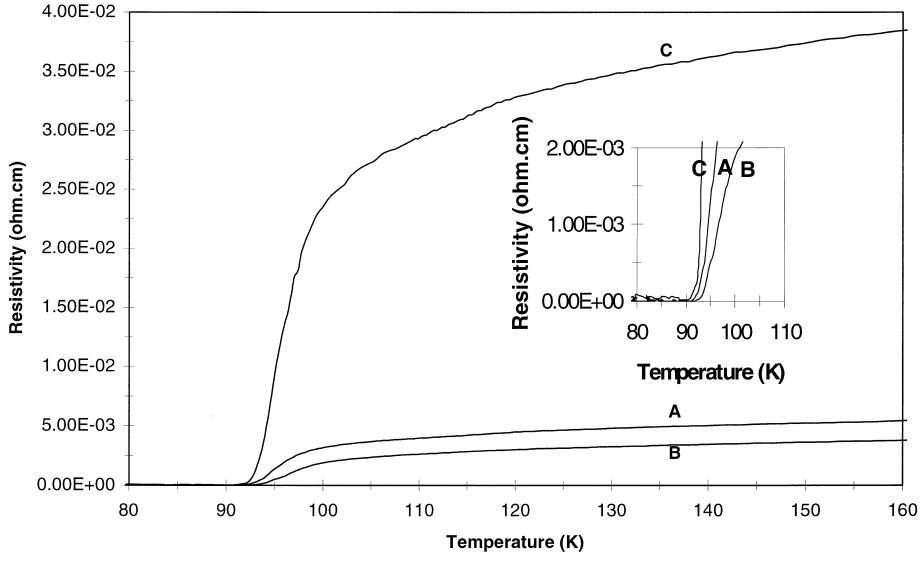

Fig. 11. Resistivity measurements vs. temperature for sinter-forged bars obtained by (A) solid state, (B) sol–gel and (C) polymer matrix methods, annealed 12 h under air at 863, 860 and 850°C, respectively.

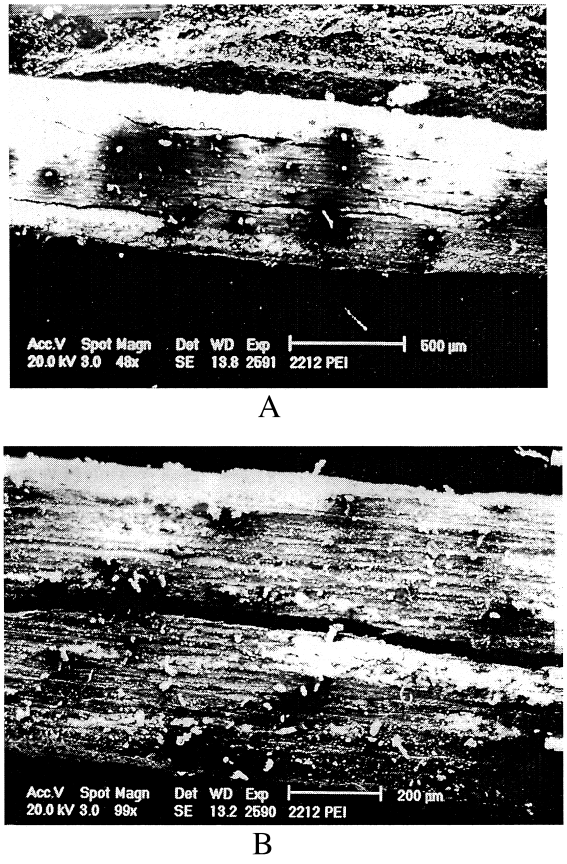

Fig. 12. SEM micrographs of annealed bars obtained by the polymer matrix method, showing the presence of big cracks all along the bar (A) and a detail of one of the cracks (B).

polymer sample only 200 A/cm^2 after annealing at 850°C, 12 h. The difference in J_c between the polymer and the other methods is in agreement with the large difference observed on the resistivity values (see Fig. 11); however, this is not due to the small difference in T_c (see Table 1), but instead may be due to the following four factors: (a) secondary phases observed in Fig. 7C; (b) the average of grain misalignment for the polymer matrix sample (17°) is larger than the other samples (14°), and the grain alignment is a very important factor for the J_c of Bi-based superconductors; (c) the bar is very thin and fragile, and small stresses can produce the breaking down or at least the damage of the bar; and (d) the existence of large cracks parallel to the bar axis (plane *ab*) that can reduce its effective section, as can be seen on micrographs shown in Fig. 12. Such cracks are not present on samples obtained by solid state or sol–gel methods.

4. Conclusion

Synthesis of high quality Bi-2212 ceramics has been done using three different synthetic methods. The polymer matrix method has been determined to be a very promising synthetic route in terms of kinetic formation and particle size (bigger platelets than those obtained by the other methods), which may allow to an easier texturation of the material under uniaxial stress. However, by using the same sinter-forging process for the three methods and in spite of similar orientation results, better J_c values were obtained for solid state and sol–gel methods. This unexpected result for the polymer matrix method is attributed to cracks which brittle the material and decrease its effective section. Nevertheless, it is confirmed that the sinter-forging process is a very effective and fast method to reorient the Bi-2212 platelets. However, the sinter-forging conditions are currently under further investigation for the polymer matrix method in order to avoid the presence of cracks, and as a consequence, to obtain good electrical properties.

Acknowledgements

The authors want to acknowledge to G. Poullain for the J_c measurements, and S. Marinel and M. Korzenski for fruitful discussions. Dr. A. Sotelo acknowledges a Marie Curie fellowship (contract No. ERBFMBICT971898).

References

[1] C. Michel, M. Hervieu, M.M. Borel, A. Grandin, F. Deslandes, J. Provost, B. Raveau, Z. Phys. B 68 (1987) 421.
[2] H. Maeda, Y. Tanaka, M. Fukutomi, T. Asano, Jpn. J. Appl. Phys. 27 (1988) L209.
[3] C.W. Chu, J. Bechtold, L. Gao, P.H. Hor, Z.J. Huang, R.L. Meng, Y.Y. Sun, Y.Q. Wang, Y.Y. Xue, Phys. Rev. Lett. 60 (1988) 941.

[4] J.M. Tarascon, Y. Le Page, P. Barboux, B.G. Bagley, L.H. Greene, W.R. McKinnon, G.W. Hull, M. Giroud, D.M. Hwang, Phys. Rev. B 37 (1988) 9382.
[5] J.L. Tallon, R.G. Buckley, P.W. Gilberd, M.R. Presland, I.W.M. Brown, M.E. Bowden, L.A. Christian, R. Goguel, Nature 333 (1988) 153.
[6] M.A. Subramanian, C.C. Torardi, J.C. Calabrese, J. Gopalakrishnan, K.J. Morrissey, T.R. Askew, R.B. Flippen, U. Chowdhry, A.W. Sleight, Science 239 (1988) 1015.
[7] A.W. Sleight, Phys. Today 44 (1991) 24, June.
[8] P. Majewski, Adv. Mater. 6 (1994) 460.
[9] N. Knauf, J. Harnischmacher, R. Müller, R. Borowski, B. Roden, D. Wohlleben, Physica C 173 (1991) 414.
[10] K. Schulze, P. Majewski, B. Hettich, G. Petzow, Z. Metallkd. 81 (1990) 836.
[11] K. Konstantinov, I. Stambolova, P. Peshev, A. Souleva, T. Tsacheva, G. Gyurov, I. Khristova, J. Anal. Appl. Pyrolysis 42 (1997) 89.
[12] V.M. Vereshchaka, A.A. Onoprienko, L.R. Shaginyan, Poroshk. Metall. 56 (1996) 27.
[13] C.L. Carvalho, D.I. Santos, E.A.A. Rubo, M.A. Aegerter, Program Ext. Abstr.-Int. Workshop Supercond. 406 (1995) .
[14] S. Li, M. Bredehöft, W. Gao, H.K. Liu, T. Chandra, S.X. Dou, Supercond. Sci. Technol. 11 (1998) 1011.
[15] M. Nevriva, V. Sima, E. Pollert, J. Chval, J. Hejtmanek, China J. Phys. 34 (1996) 320.
[16] Y. Huang, G.F. de la Fuente, A. Sotelo, A. Badía, F. Lera, R. Navarro, C. Rillo, R. Ibañez, D. Beltrán, F. Sapiña, A. Beltrán, Physica C 185–189 (1991) 2041.
[17] A. Sotelo, PhD Thesis, Zaragoza University, Spain, October 1994.
[18] V. Rouessac, J. Wang, J. Provost, G. Desgardin, Physica C 268 (1996) 225.
[19] V. Rouessac, M. Gomina, J. Eur. Ceram. Soc. 18 (1998) 81.
[20] K.H. Song, C.C. Sorrell, S.X. Dou, H.-K. Liu, J. Am. Ceram. Soc. 74 (1991) 2577.
[21] J.G. Noudem, J. Beille, D. Bourgault, A. Sulpice, R. Tournier, Physica C 230 (1994) 42.
[22] N. Murayama, E. Sudo, M. Awano, K. Kani, Y. Torii, Jpn. J. Appl. Phys. 27 (1988) L1856.
[23] A. Tampieri, G.N. Babini, Jpn. J. Appl. Phys. 30 (1991) L1163.
[24] H. Ikeda, R. Yoshizaki, K. Yoshikawa, N. Tomita, Jpn. J. Appl. Phys. 29 (1990) L430.
[25] C. Müller, P. Majewski, G. Thurn, F. Aldinger, Physica C 275 (1997) 337.
[26] P. Majewski, H.-L. Su, M. Quilitz, J. Mater. Sci. 32 (1997) 5137.
[27] V. Rouessac, J. Wang, J. Provost, G. Desgardin, J. Mater. Sci. 31 (1996) 3387.
[28] J. Fransaer, J.R. Roos, L. Delaey, O. Van Der Biest, O. Arkens, J.P. Celis, J. Appl. Phys. 65 (1989) 3277.